



two parallel data inputs is the reason that we name it parallel data convolutional codes.  $X$  and  $X'$  are two systematic outputs, whereas  $Y$  and  $W$  are two parity bits.

The data stream  $A$  and its interleaved version  $A'$  are fed into the decoder at the same time. However,  $A'$  is decorrelated relative to  $A$  due to the presence of the interleaver. For a reasonably good interleaver, like the  $S$ -interleaver used in our simulations, this should not adversely affect the performance of the code. The systematic bit  $X'$  is not transmitted as  $X'$  is the interleaved version of  $X$ . Thus, the PDCC encoder shown in Fig. 1 can typically provide a code rate of  $1/2$  by transmitting the systematic bit  $X$  and the parity bit  $Y$ , and a code rate of  $1/3$  by transmitting the systematic bit  $X$  and the parity bits  $Y$  and  $W$ . It can also provide other coding rates through puncturing the parity bits  $Y$  and  $W$  if needed.

## 2.2. Self-iterative PDCC Decoder

The key difference between the MAP algorithm for PDCCs and the MAP algorithm presented in [7] is that the PDCC encoder has two input bits and four output bits, including two systematic bits  $A, A'$  and two parity bits  $Y, W$ . The MAP algorithm described in [7], however, is applicable to the soft decoding of rate  $1/2$  systematic convolution codes which have one input bit and two output bits, including one systematic bit and one parity bit.

Assume the outputs of the PDCC encoder depicted in Fig. 1 at time index  $k$  are the systematic bit  $A_k$ , and the parity bits  $Y_k$  and  $W_k$ . These outputs are BPSK modulated and transmitted through an AWGN channel. At the receiver end, the received symbols at time index  $k$  are denoted as  $R_{A_k}$ ,  $R_{Y_k}$ , and  $R_{W_k}$ , respectively.  $A'_k$ , the interleaved version of the received symbol  $A_k$ , is obtained by interleaving  $A_k$  at the receiver, and thus will not be transmitted. It can be shown that the branch metric  $\gamma_k^{i,m}$ , which denotes the branch exiting from  $S_k = m$  with  $A_k = i$ , can be expressed as

$$\gamma_k^{i,m} = \chi_k \xi_k^i \xi_k'^j \exp \left( -L_c(R_{A_k}A_k + R_{A'_k}A'_k + R_{Y_k}Y_k + R_{W_k}W_k) \right) \quad (1)$$

where  $\chi_k$  is a constant,  $\xi_k^i = Pr(A_k = i)$ ,  $\xi_k'^j = Pr(A'_k = j)$ , and  $L_c = 2/\sigma^2$ . The likelihood ratio  $\lambda_k$  associated with each decoded bit  $A_k$  is compared to a threshold equal to one in order to determine the decoded bit  $\hat{A}_k$ .

The novelty of decoding the PDCCs lies in self-iterative decoding. The self-iterative PDCC decoder operates like a normal MAP decoder except it feeds the extrinsic outputs after interleaving or deinterleaving back as *a priori* inputs. Fig. 2 shows a schematic of a self-iterative PDCC decoder.

The inputs to the decoder are the soft outputs of a noisy channel  $L_cR_A$ ,  $L_cR_Y$  and  $L_cR_W$ , respectively. The de-

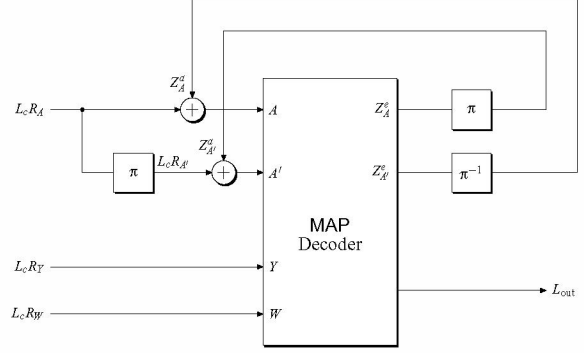


Fig. 2. Self-iterative PDCC decoder.

coder reconstructs  $L_cR'_A$  by interleaving  $L_cR_A$ . The idea of self-iterative decoding comes from the fact that  $R'_A$  is the interleaved version of  $R_A$ , so that the extrinsic information of  $R_A$  can be fed back as the *a priori* information for  $R'_A$  after interleaving and the extrinsic information of  $R'_A$  can be fed back as the *a priori* information for  $R_A$  after deinterleaving.

We denote the *a priori* information of  $R_A$  and  $R'_A$  by  $Z_A^a$  and  $Z_{A'}^a$ , while the extrinsic information of  $R_A$  and  $R'_A$  are denoted by  $Z_A^e$  and  $Z_{A'}^e$ , respectively. The self-iterative MAP decoder computes the APP of the information bit  $A$ . The LLR output of the decoder can be expressed as

$$L_{out} = L_cR_A + Z_A^a + Z_A^e + Z_{A'}^a + Z_{A'}^e. \quad (2)$$

The self-iterative PDCC decoder proceeds as follows. At the first decoding iteration,  $Z_A^a$  and  $Z_{A'}^a$  are initialised to zero. For the subsequent iterations,  $Z_A^e$  is interleaved and fed back as the *a priori* information for  $A'$ , i.e.,  $Z_{A'}^a = \pi(Z_A^e)$  where  $\pi(\cdot)$  denotes an interleaving mapping. Likewise,  $Z_{A'}^e$  is deinterleaved and fed back as the *a priori* information for  $A$ , i.e.,  $Z_A^a = \pi^{-1}(Z_{A'}^e)$  where  $\pi^{-1}(\cdot)$  denotes a deinterleaving mapping. At the final iteration, the decoder delivers the log-likelihood output  $L_{out}$ . The self-iterative decoding process can be clearly seen from the two feed back connections between  $Z_A^e$  and  $Z_{A'}^a$ , and  $Z_{A'}^e$  and  $Z_A^a$  in Fig. 2.

## 3. EXIT CHART ANALYSIS OF PDCCS

The extrinsic information transfer chart (EXIT chart) [8] is a powerful tool for analysing the convergence behavior of iterative decoding of turbo-like codes. The essential idea of the EXIT chart lies in the fact that it can predict the behavior of an iterative decoder by looking solely at the input/output relations of individual constituent decoders. The EXIT chart analyses the input/output characteristics of a single soft-input/soft-output (SISO) decoder by observing the extrinsic information at the output of the decoder for a

range of *a priori* input. It then uses mutual information to describe the extrinsic information transfer characteristics of an iterative SISO decoder.

The EXIT chart analysis is based on two empirical observations obtained by simulation. First, the *a priori* information  $A$  remains uncorrelated from the channel observations  $Z$  for large interleavers. Second, the extrinsic output  $E$  yielded by one constituent decoder approaches a Gaussian-like distribution with increasing number of iterations.

As discussed in [8], the *a priori* information  $A$  is measured in terms of mutual information  $I_A = I(X; A)$  between the transmitted systematic information bits  $X$  and  $A$  in  $L$ -values [9] as

$$I_A = \frac{1}{2} \sum_{x=-1,1} \int_{-\infty}^{+\infty} p_A(\xi|X=x) \cdot \log_2 \frac{2p_A(\xi|X=x)}{p_A(\xi|X=-1) + p_A(\xi|X=1)} d\xi. \quad (3)$$

Similarly, the extrinsic output  $E$  of the SISO decoder can also be measured in terms of mutual information  $I_E = I(X; E)$  between the transmitted systematic information bits  $X$  and the extrinsic information  $E$  in  $L$ -values as

$$I_E = \frac{1}{2} \sum_{x=-1,1} \int_{-\infty}^{+\infty} p_E(\xi|X=x) \cdot \log_2 \frac{2p_E(\xi|X=x)}{p_E(\xi|X=-1) + p_E(\xi|X=1)} d\xi. \quad (4)$$

The convergence behaviour of the iterative decoder can be described as a mapping between mutual information  $I_A$  and  $I_E$ .

In order to investigate the convergence behaviour of the self-iterative PDCC decoder depicted in Fig. 2, we apply the EXIT chart algorithm to PDCCs in this paper. The *fundamental* difference between the PDCC EXIT chart analysis and the parallel concatenated convolutional codes (PCCCs or turbo codes) EXIT chart analysis lies in the fact that generating PCCC EXIT charts does not need an interleaver, while generating PDCC EXIT charts does need an interleaver. This is because the self-iterative PDCC decoder has two received systematic channel inputs in parallel, with one systematic channel input  $L_C R_{A'}$  being the interleaved version of the other systematic channel input  $L_C R_A$  as shown in Fig. 2. As a result, we need to prepare two *a priori* inputs to the self-iterative PDCC decoder for applying the EXIT chart algorithm to the PDCC.

Assume  $x$  and  $x'$  are the two systematic information data inputs of the PDCC encoder. In the EXIT chart analysis, the two *a priori* inputs  $A$  and  $A'$  to the PDCC decoder corresponding to the two information data inputs  $x$  and  $x'$  can be modeled as follows

$$A_x = \mu_A \cdot x + n_A \quad (5)$$

$$A_{x'} = \pi(A_x) \quad (6)$$

where  $n_A$  is an independent Gaussian random variable with variance  $\sigma_A^2$  and zero mean,  $\mu_A = \sigma_A^2/2$ , and  $\pi(\cdot)$  denotes an interleaving function. Equation (6) implies that we could use an interleaver to interleave the *a priori* input for  $x$  to yield the *a priori* input for  $x'$ .

## 4. SIMULATION RESULTS

In this section, we compare the performance of the PDCCs and PCCCs by means of EXIT chart analysis.

The bit error rate (BER) performance comparison between PDCCs and PCCCs was presented in [6]. The simulation configurations were that both the PDCC and PCCC have coding rate 1/2 and a block size of 8192 random information bits. An  $S$ -type interleaver [10] with  $S$  equal to 47 was used. It was shown that the performance of PDCCs is about 0.2 dB inferior to that of PCCCs at low BERs, although the performance difference of the two codes was negligible for low  $E_b/N_0$  up to 0.6 dB.

The relatively inferior performance of PDCCs was diagnosed to be caused by the so-called “self-terminating” phenomena of the PDCC. For the PCCC, an error bit could cause the trellis path to divert from the two all-zero paths. The same bit is interleaved and fed into the second constituent encoder. That bit would not cause the diverted trellis path to re-emerge earlier. On the other hand, for the PDCC, an error causes a diversion from the all-zero trellis path. The same bit is interleaved and then fed into the same PDCC encoder. That bit could cause an earlier trellis remerge and thus self-terminating.

The PDCC performance using the BER measurement is largely dependent on the interleaver structure and size. However, the EXIT chart analysis will tell us the minimum  $E_b/N_0$  that can be achieved with an infinite size interleaver and infinite iterations. Fig. 3 graphically shows the EXIT charts for the PCCC at various  $E_b/N_0$  values, whereas Fig. 4 presents the EXIT charts for the PDCC. The PCCC used in our simulation is the original punctured rate 1/2 16-state turbo code with forward and backward polynomials (21, 37) in octal [1]. For the PCCC EXIT charts, the block size is 65536 and no interleaver is used. For the PDCC EXIT charts, an  $S$ -type interleaver with  $S$  equal to 192 is used and the block size is also 65536.

As can be seen from Figs. 3 and 4, the  $E_b/N_0$  threshold for the PCCC is around 0.6 dB, whereas the  $E_b/N_0$  threshold for the PDCC is also around 0.6 dB. Therefore, for an infinite size interleaver and infinite iterations, the EXIT chart analysis indicates that the performance of the PDCC is comparable to that of the PCCC, although the BER performance of the PDCC presented in [6] is inferior to that of the PCCC due to the “self-terminating” property of the PDCC. Future research will examine PCCCs with the constituent code in Fig. 1, to allow a fairer comparison with the code used for

the PDCC.

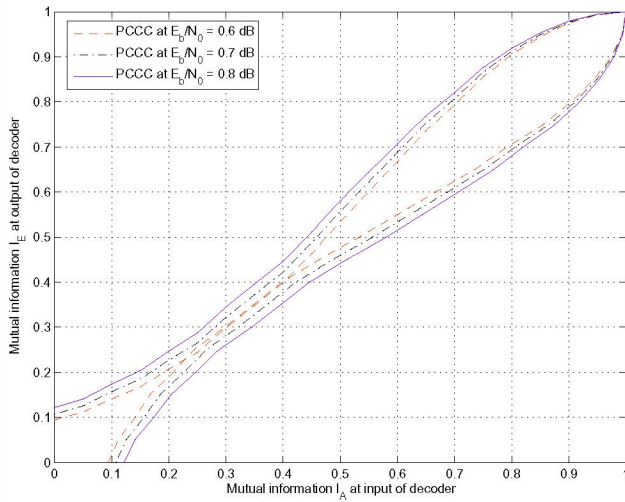


**Fig. 3.** PCCC EXIT charts with a block size of 65536.

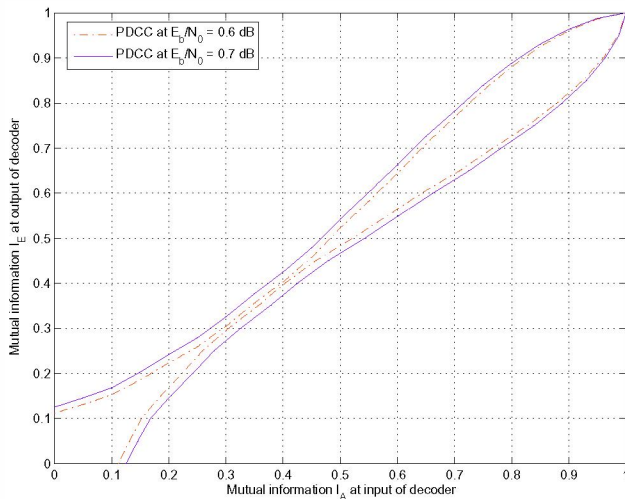


**Fig. 4.** PDCC EXIT charts with an interleaver size of 65536.

## 5. CONCLUSIONS

In this paper, the results using the EXIT chart analysis applied to PDCCs are presented. The PDCC features a parallel interleaved systematic data input and a self-iterative decoder.

Previous results by means of Monte Carlo BER simulation showed that PDCCs may have inferior performance compared to PCCCs. This is due to the PDCC's undesirable self-terminating property. Therefore, the interleaver structure and its robustness to the self-terminating phenomena has a strong influence on the performance of PDCCs using

Monte Carlo simulation. However, the EXIT chart analysis results presented in this paper reveal that the performance of the PDCC is close to that of the PCCC. Future research in this area includes designing self-terminating resilient interleavers to push the PDCC performance using iterative decoding close to its theoretic limit revealed by the EXIT chart analysis.

## 6. REFERENCES

- [1] C. Berrou, A. Glavieux, and P. Thitimajshima, "Near Shannon limit error-correcting coding and decoding: turbo-codes," in *Proc. IEEE Int. Conf. Commun. (ICC'93)*, Geneva, Switzerland, May 1993, pp. 1064–1070.
- [2] C. Berrou, M. Jézéquel, C. Douillard, and S. Kerouédan, "The advantages of non-binary turbo codes," in *Proc. IEEE Information Theory Workshop (ITW'01)*, Cairns, Australia, Sept. 2001, pp. 61–63.
- [3] C. Berrou and M. Jezequel, "Non-binary convolutional codes for turbo coding," *Electron. Lett.*, vol. 35, no. 1, pp. 39–40, Jan. 1999.
- [4] C. Berrou, C. Douillard, and M. Jezequel, "Multiple parallel concatenation of circular recursive convolutional (CRSC) codes," *Annals of Telecommunications*, vol. 54, no. 3-4, pp. 166–172, Mar.-Apr. 1999.
- [5] ETSI EN 301 790, *Digital Video Broadcasting (DVB); Interaction channel for satellite distribution systems*, ETSI reference EN 301 790, v.1.3.1, Mar. 2003.
- [6] W. Xiang and S. S. Pietrobon, "A new class of parallel data convolutional codes," in *Proc. Australian Communication Theory Workshop (AusCTW'05)*, Brisbane, Australia, Feb. 2005, pp. 78–82.
- [7] S. S. Pietrobon, "Implementation and performance of a Turbo/MAP decoder," *Int. J. Satellite Commun.*, vol. 16, pp. 23–46, Jan.-Feb. 1998.
- [8] S. ten Brink, "Convergence behavior of iteratively decoded parallel concatenated codes," *IEEE Trans. Commun.*, vol. 49, pp. 1727–1737, Oct. 2001.
- [9] J. Hagenauer, E. Offer, and L. Papke, "Iterative decoding of binary block and convolutional codes," *IEEE Trans. Inform. Theory*, vol. 42, pp. 429–445, Mar. 1996.
- [10] D. Divsalar and F. Pollara, "Multiple turbo codes for deep-space communications," in *JPL TDA Progress Report*, May 1995, vol. 42-121, pp. 66–77.